Available online at www.sciencedirect.com

ScienceDirect

IFAC-PapersOnLine 48-12 (2015) 340–345

Stability Analysis of Machining Processes Using Spectral Element Approach

Firas A. Khasawneh *

* *SUNY Polytechnic Institute, Mechanical Engineering, Utica, NY 13502, USA(e-mail: firas.khasawneh@sunyit.edu)*

Abstract: The stability analysis of machining processes is of utmost importance in order to guarantee high removal rates while at the same time maintaining acceptable surface finish and tool life. One of the key mechanisms for losing stability in machining is chatter vibration, which is a self-excited vibration due to the surface regeneration effect. This type of chatter occurs due to the variation in the dynamic cutting load between successive tool or workpiece rotations. A common approach to capture this dependency on prior states is to model the machining process using delay differential equations. Since chatter has detrimental effects on the cutting process, the ability to predict the combinations of the cutting process parameters that will result in chatter-free cutting is highly desirable. In this paper we describe how the stability of turning and milling processes can be studied using the spectral element approach. The results show that this approach can successfully predict the chatter-free regime in turning and milling. Further, we describe how recent numerical implementations of the approach to a wider class of delay equations can enable the analysis of more complex and realistic machining models.

Keywords: Machining, Spectral analysis, Stability, Time delay, Time domain analysis

1. INTRODUCTION

Conventional material removal processes such as turning and milling still constitute a large class of modern machining processes. Therefore, it is beneficial to optimize these processes such that the maximum amount of material is removed while at the same time satisfying important manufacturing constrains such as the surface quality, tool life, and noise level.

One of the most prominent problems in machining processes is regenerative chatter which is typically referred to simply as chatter (Quintana and Ciurana (2011)). These variations are the result of the phase shift between the cutting marks left on the surface between successive tool/workpiece revolutions. A well-accepted mechanism for explaining and describing chatter includes delays in the governing equation of the system. The resulting delay differential equations (DDEs), which also appear in many areas of science and engineering, have been an active topic of research for over six decades. Both frequency (Altintaş and Budak (1995); Otto et al. (2014)) and time domain (Insperger and Stépán (2004); Butcher et al. (2009); Khasawneh et al. (2012)) methods were developed to ascertain the stability of machining models. One of the recent methods that has been successfully used to study the stability of delay differential equations is the spectral element method (Khasawneh and Mann (2011a)). The spectral element approach is robust and flexible and it is capable of fast convergence as was shown in Tweten et al. (2012). Therefore, it can have useful applications in the study of machining models and delay equations in general.

In this paper the stability analysis of DDEs using the spectral element approach (SEA) is first described. We then use the SEA to study the stability of a turning and a milling model. The resulting stability diagrams, which chart the chatter and the chatter-free regime in the space of the cutting depth and the spindle speed, are presented and compared to results from the literature. The paper concludes with some available and some possible extensions for the approach.

2. STABILITY ANALYSIS WITH SPECTRAL ELEMENT METHOD

In order to simplify the presentation, we describe the stability analysis for systems of the form

$$\frac{dx}{dt} = A(t)x(t) + B(t)x(t-\tau), \tag{1}$$

where A and B are the $d \times d$ system matrices, and τ is the time delay. In this paper, we consider the autonomous ($A(t) = A, B(t) = B$) case and the non-autonomous time-periodic case ($A(t+T) = A(t), B(t+T) = B(t)$), and we study the corresponding stability of stationary solutions (autonomous case) and periodic orbits (non-autonomous case) of (1). Although the approach can be used for arbitrary T to τ ratios (Khasawneh and Mann (2013)), we restrict the presentation to the case $\tau = T$, i.e., to constrained meshes.

Since it is often impossible to deal directly with the infinite dimensional DDE (1), it must first be discretized to produce a finite dimensional approximation. The idea is that as the degree of approximation increases, the solution of the finite dimensional problem converges to that of the infinite dimensional problem. The goal of the approximation is to construct a finite dimensional dynamic map in the form

$$x_m = U x_{m-1}, \tag{2}$$

10.1016/j.ifacol.2015.09.401

where x_m and x_{m-1} are the vectors of the discretized states on $[-\tau+T, T]$ and $[-\tau, 0]$, respectively, whereas U is the monodromy matrix, which represents a finite dimensional approximation to the infinite dimensional monodromy operator. The monodromy operator U corresponds to the evolution family E of the linearized system (Diekmann et al. (1995)) evaluated in the coefficients' period T with initial instant 0, i.e., $U = E(T, 0)$. This operator maps the initial state defined on $[-\tau, 0]$ into the state one T later, $[T-\tau, T]$. The stability of the system is then investigated using the eigenvalues of U according to the criteria shown in Fig. 1.

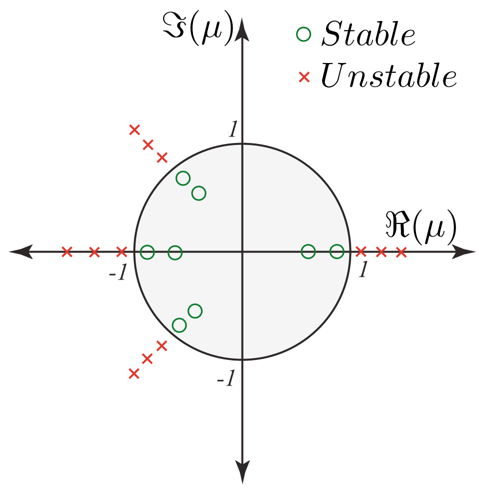

Fig. 1. The stability criteria dictates that all the eigenvalues, μ, of the monodromy operator U, should lie within the unit circle in the complex plane.

The first step for ascertaining the stability of (1) using SEA is to discretize the period $[0, T]$ using a finite number of temporal elements E. Each element is described by the interval

$$e_j = [t_j^{\mathrm{L}}, t_j^{\mathrm{R}}), \tag{3}$$

where t_j^{L} and t_j^{R} denote the left and right element boundaries, respectively, with the length of the jth element given by

$$h_j = t_j^{\mathrm{R}} - t_j^{\mathrm{L}}. \tag{4}$$

The index j starts at the leftmost element on the time line, i.e., $e_1 = [-\tau, -\tau + h_1)$. A local normalized time $\eta = \sigma/h_j$ is defined within each element where $\sigma \in [0, h_j]$ is the local time while $\eta \in [0, 1]$. The barycentric Lagrange formula is then used to obtain an approximate expression for the states over each element using $n+1$ distinct, local interpolation nodes normalized by h_j according to

$$x_j(t) = \sum_{i=1}^{n+1} \phi_i(\eta) x_{ji}, \tag{5}$$

where $x_{ji} = x_j(t_i)$ with i indicating the ith local interpolation node, and ϕ_i are the trial functions that can be calculated using the barycentric Lagrange formula in Higham (2004)

$$\phi_i(\eta) = \frac{\frac{\varpi_i}{\eta - \eta_i}}{\sum_{k=1}^{n+1} \frac{\varpi_k}{\eta - \eta_k}}, \tag{6}$$

where for node η_k the trial functions must satisfy

$$\phi_i(\eta_k) = \begin{cases} 1, & i = k \\ 0, & i \neq k. \end{cases} \tag{7}$$

while the barycentric weights ϖ_k are given by

$$\varpi_k = \frac{1}{\prod_{k \neq j} (\eta_j - \eta_k)}, \qquad j = 1, \ldots, n+1. \tag{8}$$

In this study we use (6) to obtain the trial functions since it has better numerical stability and requires less computation than the conventional Lagrange representation, see Berrut and Trefethen (2004); Higham (2004). The barycentric weights can also be used to obtain the value of the derivative of the trial functions evaluated at the interpolation nodes according to

$$\phi_i'(\eta_k) = \begin{cases} \dfrac{\varpi_i/\varpi_k}{\eta_i - \eta_k}, & i \neq k \\ \displaystyle\sum_{i=0, i \neq k}^{n+1} \dfrac{-\varpi_i/\varpi_k}{\eta_i - \eta_k}, & i = k \end{cases}. \tag{9}$$

Substituting the expression from (5) into (1) gives

$$\sum_{i=1}^{n+1} \frac{1}{h_j} \dot{\phi}_i(\eta) x_{ji} - A(t_j^{\mathrm{L}} + \eta) \sum_{i=1}^{n+1} \phi_i(\eta) x_{ji} - B(t_j^{\mathrm{L}} + \eta) \sum_{i=1}^{n+1} \phi_i(\eta) x_{(j-n_e),i} = \text{error}, \tag{10}$$

where the residual error is due to the approximation procedure while n_e indicates the number of elements used to discretize the states in $[0, T]$. We emphasize that this presentation assumes a constrained mesh and temporal elements of uniform length.

We minimize the errors in a weighted integral sense (10) (Reddy (1993)) over each temporal element. Specifically, (10) is multiplied by a set of independent weight functions $\psi_p(\eta)$ where $p = 1, 2, \ldots, n$ and is integrated over the normalized length of each element within the constrained mesh according to

$$\int_0^1 \left[\sum_{i=1}^{n+1} \frac{1}{h_j} \dot{\phi}_i(\eta) x_{ji} - A(t_j^{\mathrm{L}} + \eta) \sum_{i=1}^{n+1} \phi_i(\eta) x_{ji} - B(t_j^{\mathrm{L}} + \eta) \sum_{i=1}^{n+1} \phi_i(\eta) x_{j^*,i} \right] \psi_p(\eta)\, d\eta = 0. \tag{11}$$

In this study we chose the weight functions to be the set of the n shifted Legendre polynomials.

The weighted residual integral in Eq. (11) is often difficult to evaluate analytically. Therefore, analytical integration is substituted by a quadrature rule which uses $n+1$ quadrature points over each element, which coincide with the $n+1$ interpolation nodes, according to

$$\sum_{k=1}^{n+1} w_k \left(\sum_{i=1}^{n+1} \frac{1}{h_j} \dot{\phi}_i(\eta_k) x_{ji} - A(t_j^{\mathrm{L}} + \eta_k) \sum_{i=1}^{n+1} \phi_i(\eta_k) x_{ji} - B(t_j^{\mathrm{L}} + \eta_k) \sum_{i=1}^{n+1} \phi_i(\eta_k) x_{j^*,i} \right) \psi_p(\eta_k) = 0, \tag{12}$$

where η_k and w_k are the quadrature nodes and weights, respectively.

To construct a dynamic map, each discretization point in $[0, T]$ is mapped by τ. Since (1) is linear in x_{ji} and